Journal of Faculty of Science (Menoufia University). **Vol. 27(1)**, (2023), 152-171
Title: Reservoir characterization of the Messinian Abu Madi ...
Author: Khalifa et al

Scientific Journal of Faculty of Science (Menoufia University)

ISSN: 1110-2195

جامعة المنوفية
Menoufia University
منارة المعرفة فى قلب الدلتا

Reservoir characterization of the Messinian Abu Madi reservoir in South Abu El Naga gas field, Onshore Nile Delta, Egypt.

Mohamed A. Khalifa[a], Bassem S. Nabawy[b], Mohamed F. Abu-Hashish[a], Noha M. Hassan[a],

Ahmed W. Al-Shareif [a,c]

[a] Department of Geology, Faculty of Science, Menoufia University, El Menoufia, Egypt.

[b] Geophysical Sciences Department, National Research Centre, Cairo, Egypt.

[c] El Wastani Petroleum Company (WASCO), 5th Settlement, New Cairo, Egypt.

*Correspondence
Email: mfarouk64@gmail.com

Abstract: The main target of the present study is determination of the properties of Upper Miocene reservoirs, that help us to predict the distribution and quality of these reservoirs. The study area is located in the northeastern part of the onshore Nile Delta, between Latitudes 31° 11' 00" and 31° 15' 00", and Longitudes 31° 50' 00", 31° 53' 00", and 31° 54' 00", where the total area is approximately 8.73 Km². The present study focuses on using the available geological information, well log and core data to evaluate the Upper Miocene Abu Madi sand bodies' reservoir, through the interpretation and integration of the electrical logs with core data, to find out the connections between the geological information and the well logging deductions. The results confirm that, the sandstone content exists as a main lithology in the Abu Madi Formation, at South Abu El Naga-2 and South Abu El Naga-9 wells. The best quality sandstone appears in the Upper Abu Madi section at South Abu El Naga-9 well (SAEN-9) and in the Lower Abu Madi section at South Abu El Naga-2 well (SAEN-2). The clastics in Abu Madi formation have good physical properties, in which the central part of the study area is the best area, as net pay and quality of Abu Madi reservoir and northeastern part is lowest quality.

Journal of Faculty of Science (Menoufia University). **Vol. 27(1)**, (2023), 152-171.

-152-

1. Introduction

The Nile Delta holds immense significance as a prominent hydrocarbon province within Egypt, playing a crucial role in the country's gas production. Consequently, it remains a primary focus for ongoing and future exploration endeavors aimed at gas production (Abd El-Aal et al., 2018). Recent groundbreaking discoveries, such as the Zohr gas field, have underscored the region's remarkable potential, effectively meeting domestic natural gas demands and propelling Egypt to become a major gas exporter in North Africa and the Middle East (El-Mahdy et al., 2017). Remarkably, the Nile Delta stands as the earliest recognized delta in the world, with Herodotus documenting its existence during the 5th century AC (Said, 1981). Over time, the Nile Delta has become enveloped by a substantial sequence of Neogene clastic sediments, solidifying its status as one of Egypt's most vital gas provinces. The study area is located at in the eastern part of the Nile Delta Onshore, at the western edge of El Manzala Lake, and east of the Damietta Nile branch. The study area is located between Latitudes 31° 11' 00" and 31° 15' 00", and Longitudes 31° 50' 00", 31° 53' 00", and 31° 54' 00", in which the total area is approximately 8.73 Km² (Fig. 1). The main target of the present study is using the available geological information, well log and core data, to determine the properties of the Upper Miocene reservoirs that help us to predict the distribution and quality of these reservoirs.
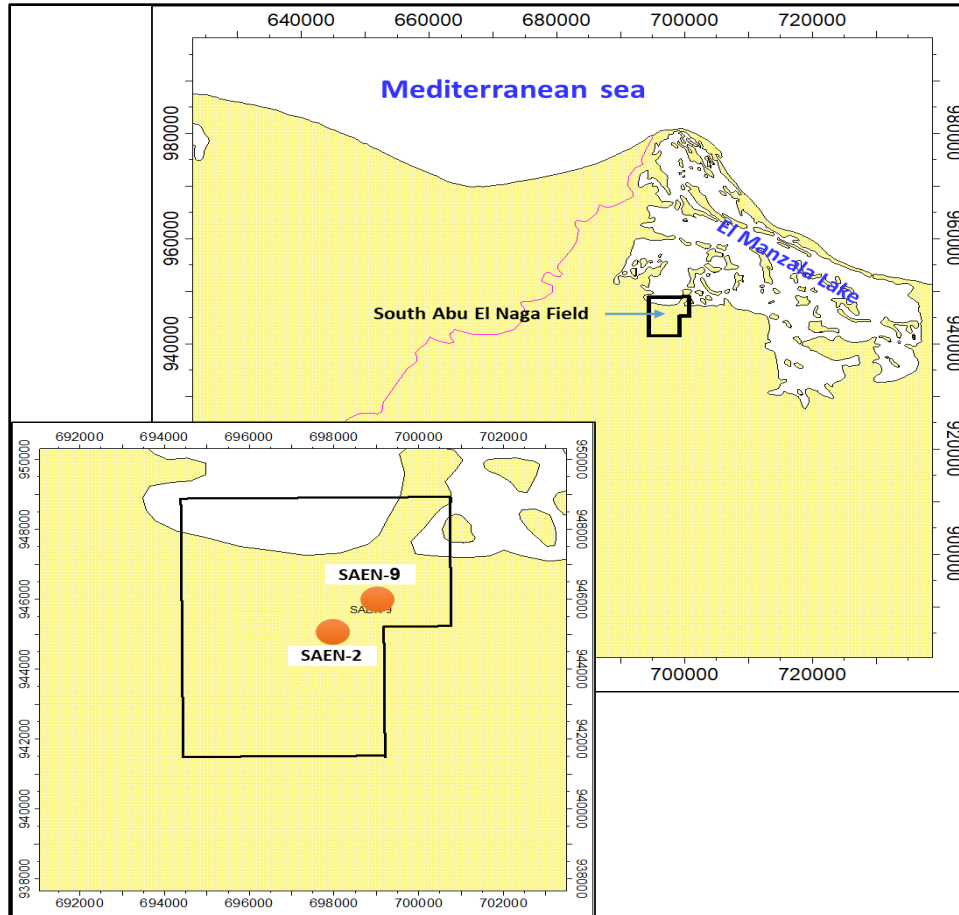
Figure 1: Location map of the onshore South Abu El Naga gas field in east of the Nile Delta.

2. Geologic Setting

The formation and development of the Nile Delta during the Late Eocene and Early Miocene periods were heavily influenced by its main tectonic features, (Said, 1990). Located at the northern frontier of the NE-African plate, which extends from the subduction zones of Cretan and Cyprus arcs to the rifted Red Sea from the Arabian plate, the Nile Delta can be divided into two provinces according to Sestini in (1995) (Fig. 2):

The Deep Offshore Nile Delta: This region experienced substantial influence from the deposition of Pliocene-Pleistocene sediments, which accumulated to a thickness of over 3500 meters

in a period of 4-5 million years. Faulting, particularly in the NNE and NE directions, became evident during the post-Messinian era.

The Onshore Nile Delta: This area is divided by a flexure zone known as a hinge line, which separates it into two primary structural sedimentary subprovinces—the North and the South Nile Delta provinces.

Since the Oligocene epoch, the present tectonic configuration of the region has resulted from the submergence of a once-emerging microcontinent during the Paleocene and Eocene, (El-Gamal and El-Bosraty, 2008). The area's structure was initially a prominent elevated region, characterized by a significant unconformity at the shoulder of the main channel in the Messinian section. The primary regional seal consisted of the Pliocene shale from the Kafr El-Sheikh Formation, (El-Maghraby et al., 2008). The clastic sediments in the Nile Delta can be classified into three major sedimentary cycles (Rizzini et al., 1978). The Miocene cycle, which lacks a well-recorded base, primarily comprises shallow marine to non-marine sediments from the Sidi Salem Formation, Qawasim Formation, and Abu Madi Formation. The Plio-Pleistocene cycle includes the marine Kafr El Sheikh Formation, as well as the deltaic El Wastani, Baltim, Mit Ghamr, and Bilqas Formations. The topmost cycle is the Holocene cycle, which can exceed a thickness of 20,000 feet and overlays Paleogene carbonates and clastic sediments. During the Messinian period (7.24 to 5.33 million years ago), the Mediterranean Sea gradually became isolated from the Atlantic Ocean, leading to widespread gypsum precipitation (5.96 to 5.6 million years ago), extensive salt deposition (5.6 to 5.5 million years ago), and a sudden drop in sea level. This drop in sea level resulted in the formation of brackish water environments known as the "Lake Sea" facies, (Roveri et al., 2014). The decrease in sea level triggered widespread erosion and the formation of large canyon incisions throughout the

Mediterranean, along with the accumulation of salt deposits in the basin's depo-center, (Dolson et al., 2005). The Messinian deposits were subsequently covered by the marine flooding of the Pliocene around 5.3 million years ago. This transgression in the Pliocene is believed to have occurred due to the reconnection with the open sea. Rifting and extension processes persisted during the Jurassic and Early Cretaceous periods, resulting in the formation of east-west trending basins. This was followed by general thermal sagging and subsidence, leading to the development of shelf margins.
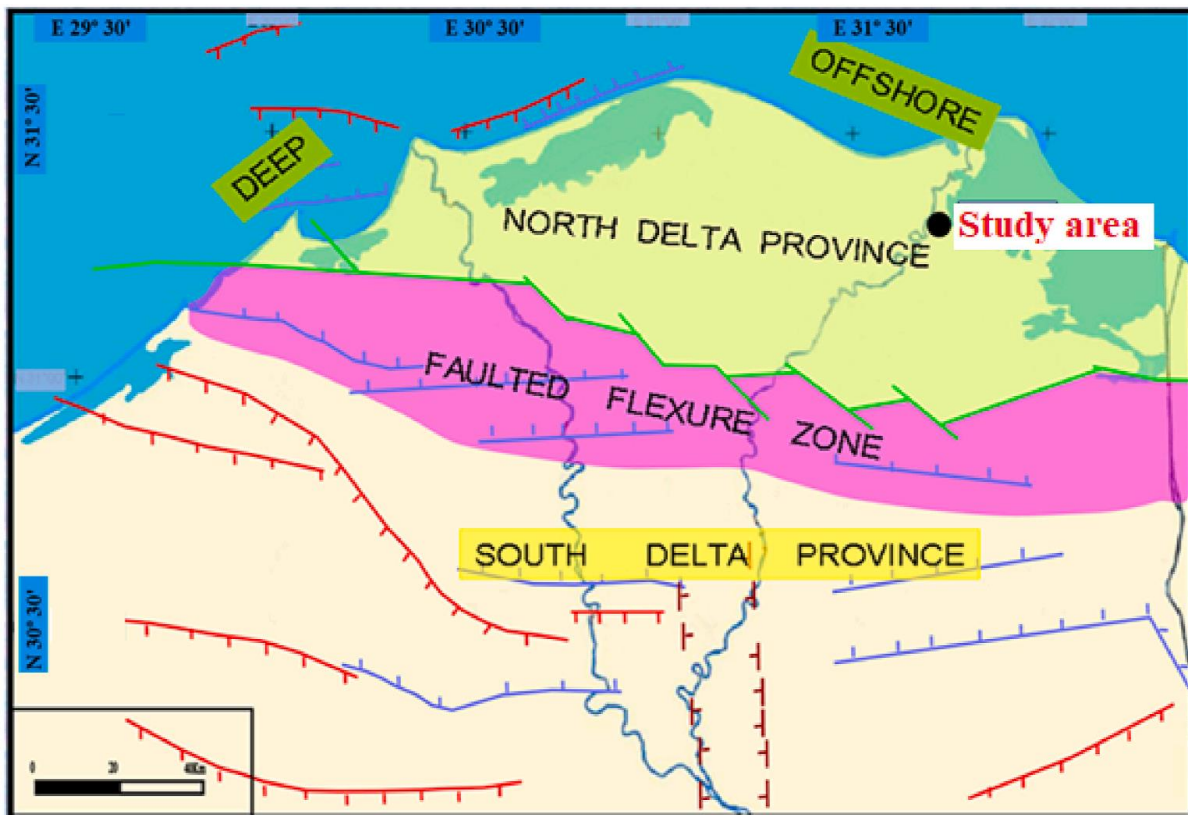

Figure 2: Schematic diagram illustrating the Main tectonic features of the Nile Delta and southeast Mediterranean region (after IEOC, 2006).

The term "Abu Madi Formation" was coined in 1974 by the National Committee of Geology Science (NCGS) to describe thick layers of sandstone and shale found in the Abu Madi-1 well, located at latitude 31°27' N and longitude 31°22' E. The formation contains loose quartz grains of

varying sizes, and conglomerate layers with an unconformity surface can be found in its lower part. The Abu Madi reservoir, known for its favorable characteristics such as good porosity (around 21%), has been the primary focus of gas field development in the Nile Delta region (Schlumberger, 1984). Determining the age of the Abu Madi Formation has been a subject of debate. In the original study location, it was observed that the formation overlies the Sidi Salem Formation in an unconformable manner (Issawi et al., 1999). Initially, it was believed to belong to the Early Pliocene epoch (Rizzini et al., 1978). However, recent research suggests that it is from the Late Miocene Messinian period, based on the presence of rare benthonic foraminifera, particularly sphaeroidinellopsis sp. The Abu Madi Formation is thought to have originated from fluvial to coastal marine environments, with its sediments deposited in a subsiding basin influenced by a transgressive sea (Rizzini et al., 1978). Hydrocarbons in the Nile Delta region have been generated by deep source rocks, with some migrating to as high as the Pleistocene in certain fields. This results in catagenetic gas being present in the Abu Madi Formation, while shallower sections commonly contain biogenic gas (Dolson et al., 2005). The geological history of the Nile Delta involves rifting and extension during the Jurassic and Early Cretaceous periods, which formed east-west trending basins. Subsequent thermal sagging and subsidence led to the development of shelf margins (Dolson et al., 2001). During the Late Cretaceous to Miocene period, the rift basins underwent inversion, creating large northeast-southwest oriented folds in the southern region of the Nile Delta and the Eastern Mediterranean (Ayyad and Darwish, 1996; Kusky et al., 2003). The tectono-stratigraphic evolution of the eastern Nile Delta is illustrated in Figure 2. The "hinge line," an Upper Cretaceous carbonate shelf edge, acts as the southern boundary for thick Neogene sediments in the Nile Delta, defining Egypt's rifted continental margin (Bertello et al., 1996). This hinge line plays a crucial role in shaping the overall stratigraphic and tectonic evolution of the Nile Delta basins. In the Oligo-Miocene period, the Gulf of Suez rift

occurred as a subsequent phase of rifting, characterized by extension along northwest faults due to the divergence of the Arabian plate from the African plate. The east-west and northwest trending faults in the Nile Delta, believed to be associated with the initial rifting stages of the Gulf of Suez, are from the Oligo-Miocene or older periods (Fig. 2).
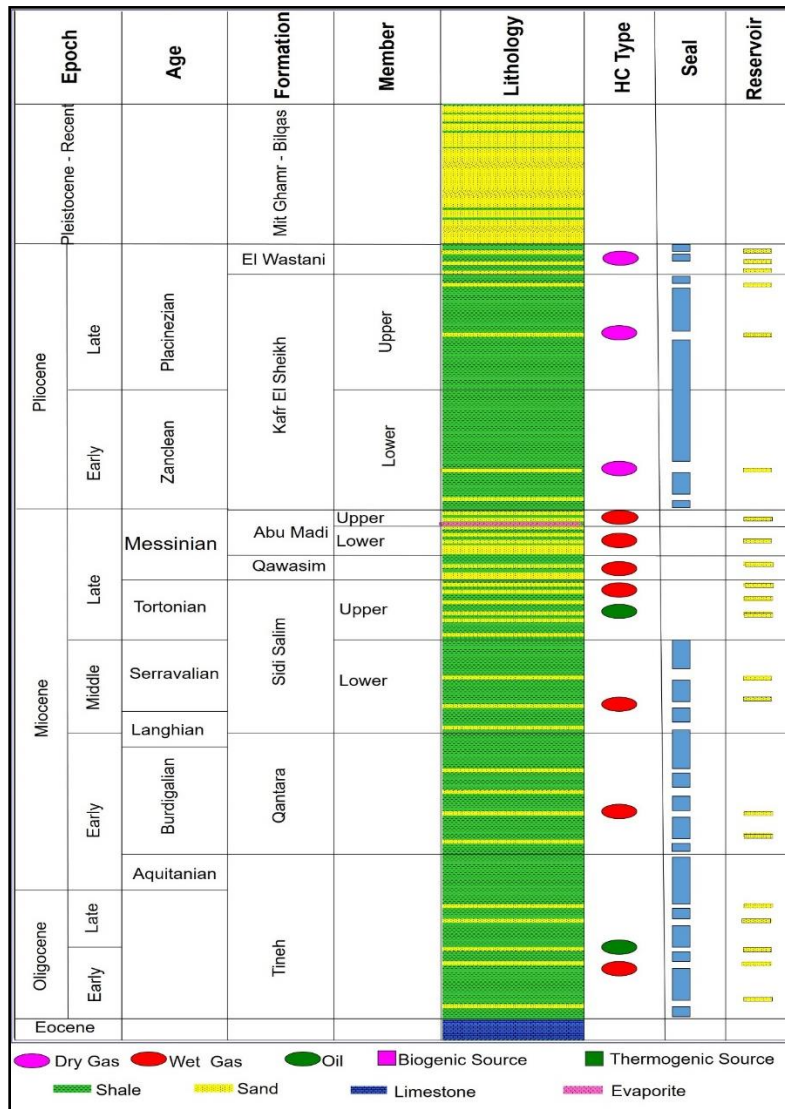

Figure 3: General view of the lithostratigraphic sequence (Eocene- Holocene) and situation of the oil and gas reservoirs throughout the sequence of onshore and offshore Nile Delta (Wasco, 2022).

3. Methodology and Available Data Sets

The primary focus of this study is to integrate core and petrophysical analysis. The dataset employed in this research consists of both well log data and core data information. The assessment of the Upper Miocene reservoirs is based on data collected from two specific wells, namely SAEN-2 and SAEN-9. A comprehensive collection of petrophysical data is available, which includes a range of electric logs such as Gamma-Ray, Resistivity, Neutron, and Density logs. These logs cover the Upper Miocene reservoirs and offer valuable insights into the physical properties of the rocks, encompassing factors such as porosity, permeability, and saturation. Additionally, X-ray diffraction (XRD) analysis was applied to 22 samples for clay fraction extracted from the core of well SAEN-2. This analysis aimed to provide detailed information on the mineralogical characteristics of the rock samples. Furthermore, the interpretation of these findings in relation to reservoir quality was also undertaken.

3.1 Petrophysical techniques

In this geological study, an analysis was conducted on two wells located in the South Abu El Naga Gas Field within the Abu Madi reservoir. The available dataset was comprehensive, consisting of conventional triple combo logs measurements specifically obtained for the Abu Madi Formation in the both wells SAEN-2 and SAEN-9, as well as core data solely from the SAEN-2 well. The objective was to conduct an analysis and determine the petrophysical parameters, including clay volume, porosity, and water saturation, based on this dataset. To achieve this, various techniques were employed to determine the appropriate petrophysical parameters and evaluate the reservoir's potential. These techniques involved the analysis of gamma-ray, neutron, density, shallow and deep resistivity measurements from the triple combo logs. Additionally, X-

ray diffraction (XRD) analysis was conducted. Cross-plots were also generated using the borehole log data to identify different clay types present in the reservoir. To facilitate the analysis of well logs and the evaluation of petrophysical properties, the Interactive Petrophysics (IP) and Techlog software were employed. These software tools played a crucial role in analyzing and interpreting the well log data, enabling a comprehensive assessment of the reservoir's petrophysical characteristics.

The determination of shale volume in this study employed two techniques: gamma-ray log as a single method and neutron-density as a double clay indicator. The equation used to calculate the shale content (Vsh) takes into account the gamma-ray logs and considers the significance of clay type and content in the evaluation process. The formula is as follows:

$$Vsh = (GR\_max - GR\_log) / (GR\_max - GR\_min) \text{ (Schlumberger, 1972)}$$

Here, GR_log represents the gamma-ray reading, GR_min is the minimum gamma-ray value, and GR_max is the maximum gamma-ray reading. Additionally, the shale volume was determined using a double technique based on the neutron-density cross-plot. The formula for this calculation is:

$$Vsh = (ØN - ØD) / (ØNsh - ØDsh) \text{ (Schlumberger, 1972)}$$

Here, ØN and ØD represent the neutron and density porosity readings of the studied reservoir, while ØNSH and ØDSH represent the neutron and density porosity in an adjacent thick shale bed, respectively.The identification of clay mineral types involved cross-plots that utilized the photoelectric effect factor (PEF) and spectral gamma-ray data (Th and K). The total porosity (ØT) was estimated as the average of neutron and density porosity values, without correcting for the

shale volume. To account for the impact of shale volume on total porosity, the effective porosity (Øe) was calculated using the following formula:

$$\text{ØT} = \sqrt{((\text{ØN}^2 - \text{ØD}^2) / 2)}$$

For a gas-bearing formation, the effective porosity (Øe.gas) was estimated based on the corrected values of both neutron and density porosities (ØNC and ØDC, respectively) using the formula:

$$\text{Øe.gas} = \sqrt{((\text{ØNc}^2 - \text{ØDc}^2) / 2)}$$

To determine the net-pay reservoir thickness, knowledge of shale volume, effective porosity, and water saturation is required. In this study, the Indonesian model, which is recommended by several authors for shaly sand interpretations, was used to calculate water saturation. This model relates deep resistivity to formation parameters such as Rw (resistivity of formation water), Rsh (shale resistivity), Sw (formation water saturation), and Vsh (shale volume). The formula for calculating water saturation (SW_Indonesia) is as follows:

$$\text{SW\_Indonesia} = \sqrt{(1/Rt)} / ((\text{Vsh}^{(1-0.5\text{Vsh})} / \sqrt{Rsh}) + \sqrt{(\text{Øe}^m / (a * Rw)))^{((2/n))}} \text{ (Poupon and}$$

Leveaux, 1971)

Here, a represents the lithology factor, m is the porosity exponent, n is the saturation exponent, Øe is the effective porosity, Sw is the formation water saturation, Rt is the formation true resistivity, and Rsh is the shale resistivity.

3.2. X-ray diffraction techniques

X-ray diffraction (XRD) analysis technique was employed to study the subsurface formation. Twenty-two samples were selected for X-ray diffraction analysis (XRD) from SAEN-2 well for detailed mineralogical analysis within the depth interval of 2304-2336m, and to determine the prevalent clay types within the formation. Organic remains were eliminated by treating the samples with 35% hydrogen peroxide (H202). The ground samples were mixed with distilled water and subjected to ultrasonic waves for clay disaggregation. The clay fraction was separated, heated, and glycolated for mineral identification based on the XRD pattern. A semi-quantitative analysis was conducted to determine the mineral composition of the isolated clay fraction, aiding in the identification of the predominant clay types in the analyzed samples.

4. Results

4.1. X-Ray Diffraction Analysis (XRD) and Clay Mineralogy:

The XRD analysis was conducted on selected 22 samples to estimate the clay mineral types present. The XRD data obtained from the SAEN-2 well showed the abundance of quartz, feldspars, calcite, kaolinite, and smectite within the Abu Madi Formation (Table 1 and fig. 4). The analysis indicates that the sand grains are predominantly composed of quartz (60-90%, Table 1), with minor percentages of feldspar, calcite, smectite, illite, and kaolinite. Generally, the clay minerals content (smectite and illite) is below 20% in most samples, except at depths of 2322 m, 2330.5 m, and 2335 m (60%, 37%, and 25% respectively, Table 1). Smectite content increases with depth and represents the dominant clay mineral type in the studied samples (Table 1). The higher clay

minerals content at the base of the Abu Madi reservoir may be attributed to the intense alteration and breakdown of feldspars into clays at this level.

Table 1: Semi-quantitative relative abundance of the minerals in the studied Abu Madi samples from South Abu El Naga Gas fields.

| S.No.	Depth (m)	Quartz %	Feldspar %	Calcite %	Smectite %	Illite %	Kaolinite %
1	2304	77	7	5	5	----	6.1
2	2307	78	5	5	6.8	----	5.2
3	2310	87	3	5	3	----	2
4	2313	89	3	3	3	----	2
5	2316	90	----	10	----	----	----
6	2319	71	19	3	5.6	----	1.4
7	2320	70	19	3	6	----	2
8	2321	74	14	2	3	1	6
9	2322	35	5	0	39	----	21
10	2323	76	7	4	9.1	----	3.9
11	2324	70	15	----	9.8	----	5.3
12	2325	83	5	4	5	----	3
13	2326	84	3	----	4.9	3.1	4.9
14	2327	83	8	----	5.4	----	3.6
15	2328	79	9	----	4.3	3.4	4.3
16	2330.5	43	20	----	20.7	----	16.3
17	2331	64	20	----	8	----	8
18	2332	61	25	----	7	----	7
19	2333	63	20	----	9	----	8
20	2334	60	21	----	10.6	----	8.4
21	2335	60	15	----	15	----	10
22	2336	80	10	----	6	----	4
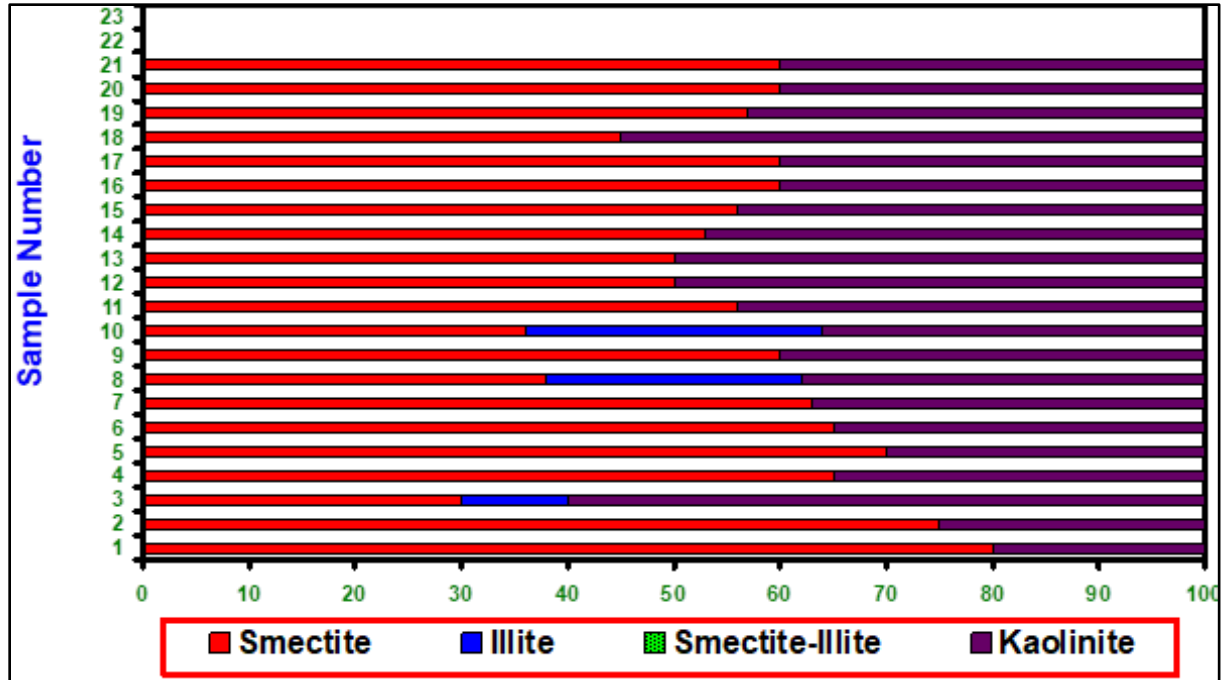
Figure 4: Schematic semi-quantitative XRD data of the clay fraction in SAEN-2 well samples.

4.2. Reservoir quality and lithology identification:

Various techniques, including mud logging and well logging, are employed to interpret subsurface lithology during drilling operations. Well logging, in particular, is the prevalent method for geophysical data acquisition in subsurface geological analysis (Bonner et al., 1992). The interpretation of well logging data encompasses a wide range of methods that involve both qualitative evaluation (such as cross-plots evaluation and electrical logging evaluation) and quantitative evaluation (petrophysical evaluation), allowing for a comprehensive analysis of the subsurface lithology.

4.2.1. Cross-plot Technique:

This section describes the evaluation of the electric log data for the studied wells SAEN-2 and SAEN-9, to identify the lithology and to determine the reservoir parameters. The qualitative evaluation is represented by the Cross-plot technique, with plotting the data points of two or more than different log data. The Neutron – Density cross-plot is the best method for the Upper Miocene lithological identification. The neutron-density cross plots of the Abu Madi formation in SAEN-2

and SAEN-9 wells, demonstrating that the major reservoir lithology in Abu Madi is sandstone with shale intercalation, the red circle refers to gas effect. (Fig. 5).
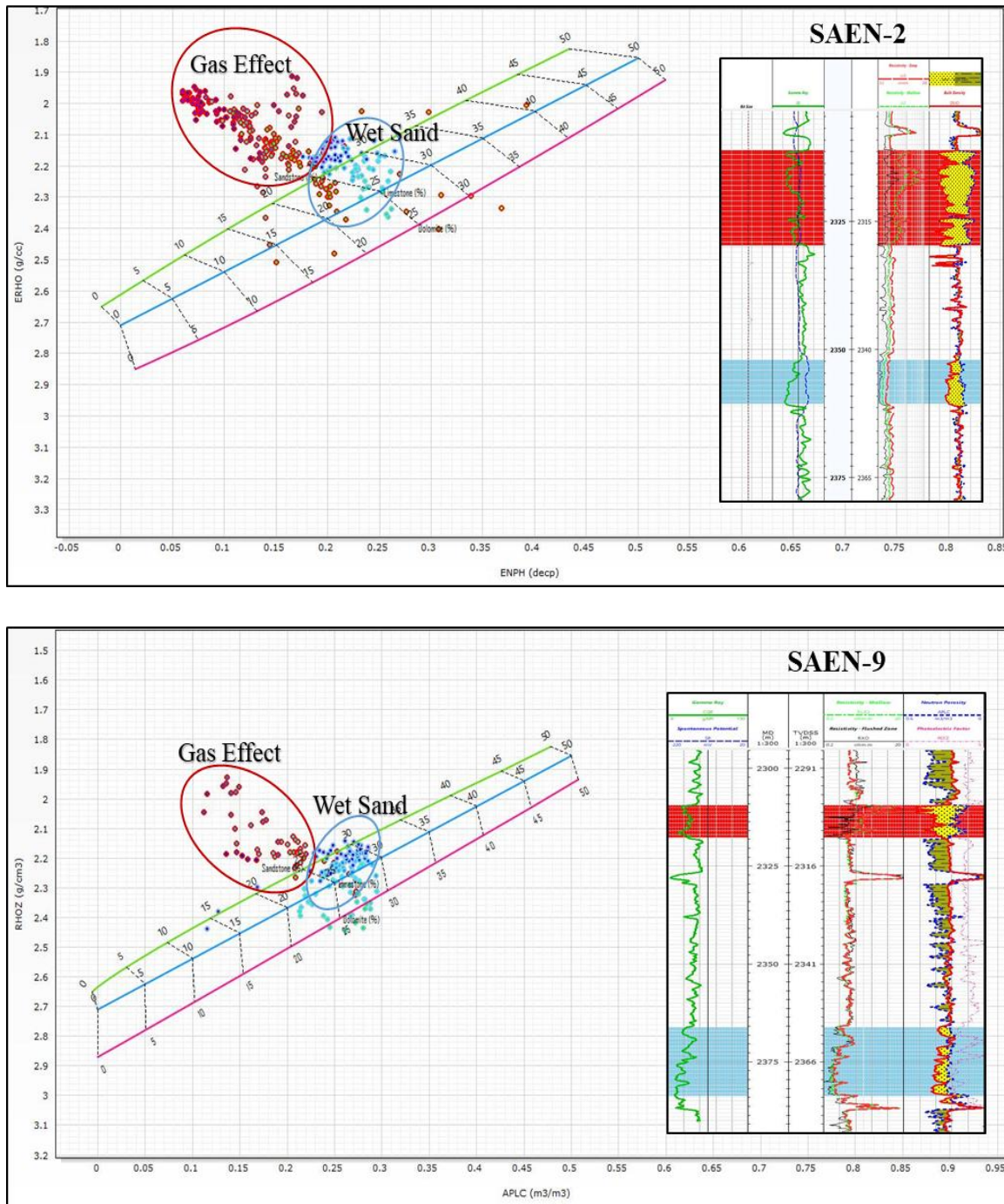

Figure 5: X-plot correlation between neutron (APLC) & bulk density (RHOZ) in Abu Madi pay and wet zones intervals in SAEN-2 and SAEN-9 wells.

4.2.2. Clay Type:

The clay type was identifying via the spectral GR (TH & K) X-plots, which indicate the predominance of the mixed Layer and illite clay minerals in SAEN-9 well, whoever, dominance of mica clay minerals in SAEN-2 well (Fig. 6). This can highlight the importance of the effect of the type of clay in determining the reservoir quality between the two wells.
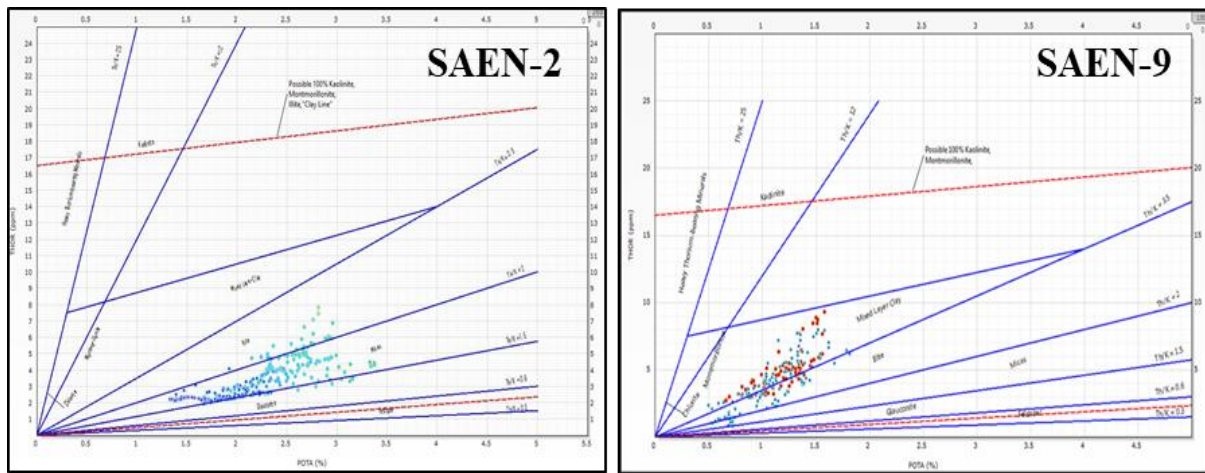

Figure 6: X-plot between thorium & potassium illustrating clay minerals type of the Abu Madi Formation in SAEN-2 and SAEN-9 wells.

4.2.3. Electric Log Interpretation and Petrophysical Evaluation:

Gamma-ray logs are utilized for qualitative evaluation in order to distinguish between shale and sandstone, as shales exhibit relatively high gamma-ray values while sandstone yields low values. Neutron, density, and photoelectric logs are employed for lithological determination. The behavior of density and neutron logs is considered the most reliable indicator of reservoir rock quality, with density moving to the left (lower density) and touching or crossing the neutron curve. A drop in the gamma-ray log and separation between the three resistivity curves correspond to these cases, respectively. A greater crossover between density and neutron indicates better reservoir quality, while the separation between density and neutron signifies the occurrence of gas, and the separation between Rxo and Rt indicates the presence of hydrocarbons. Figures 7 illustrate the lithological interpretation and reservoir quality, identified based on the different behaviors and values of density, neutron, gamma-ray, and the three resistivity curves. Intervals highlighted in

yellow represent good-quality sandstone for the Abu Madi reservoir, while other intervals indicate poor quality. The quality of the Abu Madi reservoir improves in the SAEN-2 well with a good reservoir thickness, and decreases in the SAEN-9 well (yellow-colored intervals). The re-evaluation of the Upper Miocene reservoir was conducted using interactive petrophysics (IP3.6) and Techlog (2020.2) software. The interpretation of the Abu Madi reservoir was performed using the following cutoff parameters: Vsh < 40% and Φ > 10%. Table 2 presents the main petrophysical characteristics of the Abu Madi reservoir (net pay thickness, effective porosity, and water saturation) in the two evaluated wells in the study area. The raw and conditioned logging curves are shown at tracks one, 4, and 5. The results of petrophysical analysis are shown in tracks 6, 7, and 8. However, track 6 presents the reservoir (which is shaded in yellow) & net pay (which is shaded in red), track seven presents' effective water saturation (light blue color) and gas saturation (which is shaded in red) and track 8 shows effective porosity. The average reservoir parameters in the study area are as follows:

Abu Madi reservoir in SAEN-2 well exhibits a good average effective porosity of 25% and low to medium water saturation with an average of 32%.

Abu Madi reservoir in SAEN-9 well shows good effective porosity values with an average of 27.5% and water saturation average of 39.5%.

The obtained reservoir parameters of the SAEN-2 and SAEN-9 wells are listed in Table 2.

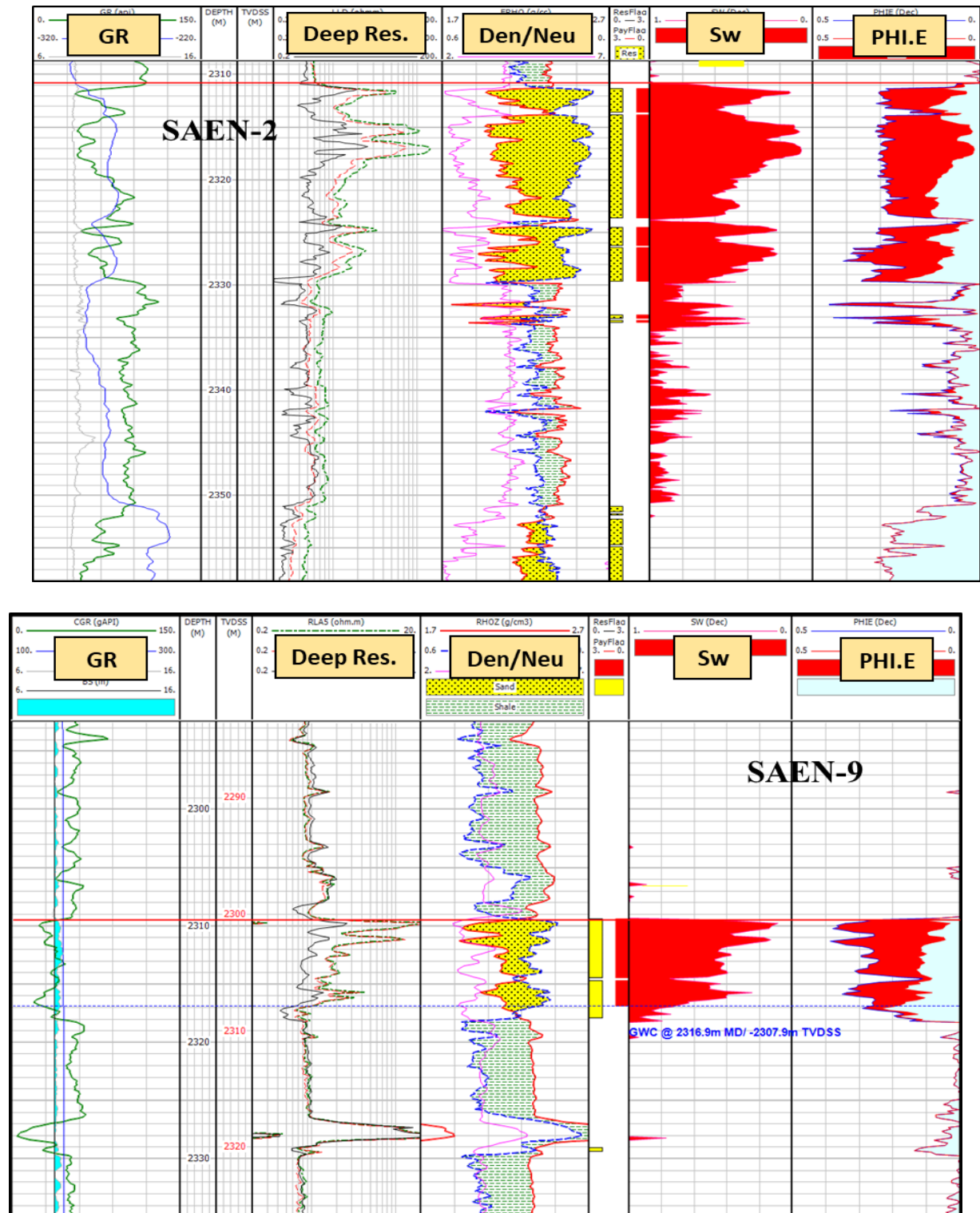| Well	Formation	Net pay (m)	Av Phi %	Av Sw %
SAEN-2	Abu Madi	16.6	25	32
SAEN-9	Abu Madi	7.3	27.5	39.5

Figure 7: Comprehensive petrophysical assessment of Abu Madi Formation in SAEN-2 and SAEN-9 wells.

Note: GR/ CGR (gamma ray), LLD/ RLA5 (deep resistivity), ERHO/ RHOZ (density), ENPH/ APLC (neutron), Sw (water saturation) and PHI.E (effective porosity).

5. Discussion and Conclusions:

The primary objective of this study is to provide a comprehensive reservoir characterization of the Messinian Abu Madi reservoir located in the South Abu El Naga gas field. The characterization involves determining reservoir quality and identifying lithology through the utilization of cross-plot techniques, analysis of electric logs, and examination of core data. The aim is to obtain a thorough understanding of the reservoir properties specific to the Abu Madi clastics in the study area, focusing on the SAEN-2 and SAEN-9 wells.

The interpretation of well logs, particularly in terms of litho-saturation cross-plots, reveals that the Abu Madi Formation primarily consists of sandstones interspersed with shales and siltstones. Within these formations, thick pay zone sandstones are more prevalent in the SAEN-2 well compared to the SAEN-9 well. Both wells exhibit high porosity, yet the SAEN-9 well demonstrates a higher proportion of water-saturated sandstones in comparison to the SAEN-2 well. Additionally, when examining spectral gamma ray (TH & K) cross-plots, differences in clay content become apparent. The SAEN-9 well indicates a predominance of mixed layer and illite clay minerals, while the SAEN-2 well displays a dominance of mica clay minerals.

The pay zone sandstones are primarily composed of quartzose material, with minimal amounts of clays and carbonate cements. Porosity values in these sandstones range from 20% to 30%. The smaller thickness of pay zones observed in the SAEN-9 well suggests that hydrocarbon accumulations in the South Abu El Naga gas field are more concentrated in the central part of the study area rather than the northeast portion. By considering these findings, it may be possible to enhance the productivity of the Messinian gas reservoir in the Onshore Nile Delta.

Acknowledgement

References

Abd El-Aal, H.A., Soliman, A.M., El-Nady, M., and El-Sayed, M.M., 2018. The hydrocarbon potential of the Nile Delta: A review. Journal of African Earth Sciences, 142, pp.131-143.

After IEOC-WASCO 2006: Structural Sketch Map of the Main tectonic features in the Nile Delta and southeast Mediterranean region on El Wastani Petroleum Company (WASCO) and International Egyptian Oil Company (IEOC) Regional study (Internal Report).

After WASCO 2022: Regional study of the Upper and Lower Messinian sequence on El Wastani Petroleum company (WASCO) development leases (Internal Report).

Ayyad, M.H., M. Darwish, 1996. Syrian Arc structures: a unifying model of inverted basins and hydrocarbon occurrences in North Egypt. Egyptian Geological Petroleum Company Seminar, November 1996, Cairo, p. 19.

Bertello, F., Barsoum, K., Dalla, S., Guessarian, S., 1996. Temsah Discovery: a Giant Gas Field in a Deep Sea Turbidite Environment. In: 13th EGPC Petroleum Conf Explor, Cairo, Egypt.

Bonner, S.; Clark, B.; Holenka, J.; Voisin, B.; Dusang, J.; Hansen, R.; White, J. and Walsgrove, T. (1992): Logging While Drilling: A Three-Year Perspective. Oilfield Review 4, no.3.

Dolson JC, Boucher, PJ, Siok J, Heppard PD (2005): Key challenges to realizing full potential in an emerging giant gas province: Nile Delta/Mediterranean offshore, deep water, Egypt. In: Dore AG, Vining BA (ed) 6th Petroleum Geology Conference, London, United Kingdom.

Dolson, C. J.; Shaan, V. M.; Matbouly, S.; Harwood, C.; Rashed, R. and Hammouda, H. (2001): The petroleum potential of Egypt. – In: Downey, W.M.; Threet, C. J. and Morgan, A.W. (Eds.): Petroleum provinces of the twenty-first century., AAPG Memoir No. 74, 453-482, American Association of Petroleum Geologists, Tulsa, Oklahoma.

El-Mahdy, M.G., El-Kaliouby, B.M., and El-Ghareeb, H.A., 2017. Petrophysical evaluation and characterization of the Zohr gas field, offshore Nile Delta, Egypt. Journal of Petroleum Science and Engineering, 155, pp.881-893.

Issawi, B., El Hinnawi M., Francis, M., Mazhar, A. (1999). The Phanerozoic Geology of Egypt. A geodynamic Approach - Egypt Geol. Surv. Special Publication 76, p. 461.

Kusky TM, Abdelsalam M, Tucker R, Stern RJ (2003). Evolution of the East African and related Orogens, and related Orogens, and the assembly of Gondwana. Spec Issue Precambr Res 123:81–344.

Poupon, A., Leveaux, J., 1971. Evaluation of water saturation in shaly formations. In: SPWLA 12th annual logging symposium, 1-2.

Rizzini, A., Vezzani, F., Coccocetta, V., & Milad, G. (1978): Stratigraphy and Sedimentation of Neogene-Quaternary section in the Nile Delta area, Egypt - Marine geology 27: p. 327-348.

Roveri, M., Manzi, V., Bergamasco, A., Falcieri, F., Gennari, R., Lugli, S., Schreiber, B.C., 2014b. Dense shelf water cascading and Messinian canyons: a new scenario for the Mediterranean

salinity crisis. American Journal of Science. 2014, 314 (3) 751-784; DOI: 10.2475/05.2014.03.

Roveri, M., Flecker, R., Krijgsman, W., Lofi, J., Lugli, S., Manzi, V., ... & Sierro, F. J. (2014). The Messinian Salinity Crisis: Past and future of a great challenge for marine sciences. Marine Geology, 352, 25-58.

Said, R., 1990. The Geology of Egypt. Balkema, Rotterdam, p. 734.

Said, R. (1981): The Geological Evolution of the River Nile. Springer, Texas, USA, p. 151.

Schlumberger (1972): The Essentials of Log Interpretation Practice Services Techniques Schlumberger, France, 58 p.

Schlumberger (1984): Well Evaluation Conference, Egypt: Geology of Egypt: p. 1-64.